

## Blended paper: physical, optical, structural, and interfiber bonding analysis

Matheus Felipe Freire Pego<sup>1</sup>✉\*, Maria Lúcia Bianchi<sup>1</sup>id

<sup>1</sup>Federal University of Lavras, Lavras, Minas Gerais, Brazil

### TECHNOLOGY OF FOREST PRODUCTS

#### ABSTRACT

**Background:** Blended paper can present suitable mechanical properties due to sinergetic effect. However, regarded to physical properties, few studies are conducted. This study aimed to evaluate optical, structural, interfiber bonding, and other physical properties from blended paper and try to understand how these properties can affect applications. The eucalyptus, sisal, and pine pulp were used for handsheet forming. Pulpes were disintegrated, refined, and blended two by two in 5/95%, 25/75%, and 45/55% ratios. Also, virgin pulps (100% of each pulp) were used for handsheet forming. Handsheets were formed and evaluated by bond strength, cobb test, air permeance, roughness, optical, Fourier transform infrared spectroscopy (FTIR), and scanning electron microscopy (SEM).

**Results:** Treatments differed statistically in bond strength, cobb test, optical, air permeance, and roughness. Generally, treatments with eucalyptus presented higher bond strength, brightness, and air permeance. Treatments with sisal presented the highest opacity and roughness. Spectra of virgin handsheets presented differences in 2170-2000 and 2360  $\text{cm}^{-1}$  bands, probably related to residual lignin content. SEM images revealed structural differences between blended and virgin pulps.

**Conclusion:** Treatment T15 (45S 55P) presented the best results, suggesting better physical-mechanical properties. Blended handsheets presented better properties than virgin handsheets on most properties, evidencing a synergetic effect.

**Keywords:** Natural fibers, Fiber mixture, Pulp quality, Pulp strength

#### HIGHLIGHTS

The fiber blending caused changes in paper properties due to fiber morphology.  
Blended paper presented a synergetic effect, higher than virgin paper.  
Eucalyptus treatment presented the highest bond strength, brightness, and air permeance.  
Analyses revealed structural differences between blended and virgin paper

.  
.

PEGO, M. F. F.; BIANCHI, M. L.. Blended paper: physical, optical, structural, and interfiber bonding analysis. CERNE, v. 27, e-102944, doi: 10.1590/01047760202127012944

✉ Corresponding author e-mail: matheusfelipefreire@gmail.com Received: 11/05/2021 Accepted: 07/10/2021



## INTRODUCTION

Paper industries are an important sector in the economy of many countries. As well as other industries, they are facing demands regarding sustainability, efficiency, and product quality (Schneider et al., 2016). This scenario leads to a constant search for improvements. One possibility to improve paper quality is through fiber blending.

Fiber blending is a paper production technique based on the combination and mixture of different fibers. Instead of an isolated fiber, the fibers are blended in different combinations to improve paper properties, reducing drawbacks and potential advantages that one fiber can present (Mansfield et al., 2004; Claramunt et al., 2020). Compared to virgin pulps, blended pulps can present higher physical-mechanical properties and induce a synergetic effect (Karlsson, 2010).

Physical properties are essential for paper application. For example, optical attributes are requested for writing and printing paper; structural and surface attributes influence fiber arrangement and mechanical properties (Biermann, 1996). When exposed to some requirements, these properties involve the paper behavior, enabling the structure characterization, arrangement, surface, and fibers connections. As well as other paper properties, physical properties can be strongly affected by fiber blending due to significant variations in fiber characteristics (Cit, 2013). Therefore, physical properties need to be considered in studies involving fiber blending.

Interfiber bonding plays an important role in paper structure (net formation, arrangement) and mechanical properties, especially tensile strength. They can be defined as connections between fibers through chemical bonding, Van der Waals' interaction, and molecular entanglement. The fibers are kept together, contributing to the paper cohesion (fiber network) and, consequently, to the physical and mechanical properties (Retulainen et al., 1997). Therefore, the evaluation of interfiber bonding is an important property that can affect fiber blending. Since fiber blending deals with distinguished fibers, a consequence in paper structure is expected. The short fiber addition in long fiber pulps can dramatically improve interfiber bonding when compared to virgin pulps. Short fiber may act as fines in the paper structure, enhancing bonding between long fibers (Yan and Li, 2013; Kimura et al., 2020).

All paper applications require a minimum amount of interfiber bonding. For example, packaging and special paper require high bond strength. Generally, interfiber bonding can be improved by two methods: adding different furnishes and by fiber treatment. Both methods intend to improve fiber connections through different methods. Interfiber bonding could also be improved by pulp refining, additives, and fines additions (Vainio and Paulapuro, 2007).

Most researches involving fiber blending seek improvements in mechanical properties (Zhang et al., 2011; Sheikhi et al., 2013; Bhardwaj et al., 2019). Regarding physical properties, structure, and interfiber bonding, few studies aimed at associating these results to mechanical properties, besides understanding the influence on applications.

Therefore, this study aimed to evaluate the physical and structural properties of blended paper and understand the connection between different fibers (eucalyptus, sisal, and pine) in paper structure.

## MATERIAL AND METHODS

### Material and handsheet forming

Cellulosic commercial pulps of eucalyptus (*Eucalyptus* sp.), sisal (*Agave sisalana*), and pine (*Pinus* sp.) were used for fiber blending and paper forming. Pulps were provided by Lwarcell and Klabin companies in the shape of cellulose sheets.

The pulps were soaked with distilled water for 48 hours to improve fiber swelling and hydration. 10 L of water (2% consistency) was used. The pulps were then disintegrated in the REGMED D-3000 disintegrator. Each pulp was subjected to refining in the REGMED HV-10 refiner. Refining time was 30, 45, and 45 minutes for eucalyptus, sisal, and pine, respectively, determined by refinability pre-tests. The pulps reached approximately 25 °SR in ideal refining time. After refining, pulps were blended considering all possible material combinations in 5/95%, 25/75%, and 45/55% ratios. Virgin pulps from each material (eucalyptus, sisal, and pine) were used for handsheet forming, totalizing 21 treatments, as described in Table 1. The pulp blending was based on volume. A mechanical stirrer FISATOM 713d model was used for blending.

Handsheets were formed based on 2% consistency and grammage around 60 g/m<sup>2</sup>. The TAPPI 205 (2002) standard and a REGMED F/SS-2 paper-making machine were used for handsheets forming. Three handsheets were formed for each treatment and evaluated.

**Tab. 1** Percent composition of the cellulose pulps in each treatment.

Treatment	Blending composition
T1 (100E)	100% eucalyptus
T2 (100S)	100% sisal
T3 (100P)	100% pine
T4 (5E 95S)	5% eucalyptus e 95% sisal
T5 (25E 75S)	25% eucalyptus e 75% sisal
T6 (45E 55S)	45% eucalyptus e 55% sisal
T7 (5E 95P)	5% eucalyptus e 95% pine
T8 (25E 75P)	25% eucalyptus e 75% pine
T9 (45E 55P)	45% eucalyptus e 55% pine
T10 (95E 5S)	95% eucalyptus e 5% sisal
T11 (75E 25S)	75% eucalyptus e 25% sisal
T12 (55E 45S)	55% eucalyptus e 45% sisal
T13 (5S 95P)	5% sisal e 95% pine
T14 (25S 75P)	25% sisal e 75% pine
T15 (45S 55P)	45% sisal e 55% pine
T16 (95E 5P)	95% eucalyptus e 5% pine
T17 (75E 25P)	75% eucalyptus e 25% pine
T18 (55E 45P)	55% eucalyptus e 45% pine
T19 (95S 5P)	95% sisal e 5% pine
T20 (75S 25P)	75% sisal e 25% pine
T21 (55S 45P)	55% sisal e 45% pine

## Bond strength

The bond strength among fibers was evaluated following the methodology proposed by Page (1969), which relates paper strength properties and fiber characteristics, shown in equations 1 and 2. Where: B= Bond strength index (N/mm<sup>2</sup>); T= Handsheet tensile strength – Breaking length (km); Z= Zero-span tensile strength – Breaking length (km); A= Average fiber cross section (cm<sup>2</sup>); g= Gravity acceleration (m/s<sup>2</sup>);  $\rho$  = Cell wall density of fiber (g/cm<sup>3</sup>); P= Fiber cross section perimeter (cm); L= Fiber length (cm); RBA= Handsheet relative bonded area (%); So= Light scattering coefficient of unbound fiber network (m<sup>2</sup>/kg); S= Light scattering coefficient of handsheet (m<sup>2</sup>/kg).

$$B = \frac{96 A \rho g Z T}{(8Z-9T)P L RBA} \quad [1]$$

$$RBA = \frac{S_o - S}{S_o} \quad [2]$$

Some items were considered constant in bond strength determination. The values of 9.80665 m/s<sup>2</sup> and 1.53 g/cm<sup>3</sup> were designed for gravity acceleration (g) and cell wall density ( $\rho$ ), respectively. Parameters related to tensile strength (T and Z) and morphological properties of fibers (L, P, A) were measured in the laboratory. The formed handsheet were tested by tensile properties according to TAPPI T 494 (2006) standard for each treatment. The TAPPI T 220 (2001) was used for handsheet density and grammage. Fiber morphology was measured in Ken-A Vision optical microscope, model TT-1010, Dinocapture 2.0 software. Only measurements of virgin refined pulps (T1, T2, and T3) were conducted. Mean values from each pulp were obtained, and then the other treatments were calculated according to fiber type percentage.

RBA was calculated based on the method proposed by Tao and Liu (2011), who developed a method to determine sheet relative bonded area using the fiber flexibility index (FFI) and obtained relevant results between calculated and measured RBA. FFI was obtained by equation 3. RBA was obtained by equation 4, using FFI.

$$\text{Sheet density} = 5.5887E - 17 * (FFI) + 342.67 \quad [3]$$

$$RBA = 8.045E - 20 * (FFI) + 0.4935 \quad [4]$$

## Fourier Transform Infrared Spectroscopy

Infrared spectroscopy analysis (FTIR) was carried out to observe and identify possible chemical structures in the paper. FTIR was performed only for virgin pulp handsheets (T1, T2, and T3) due to negligible differences in spectra for blended paper, as previously evaluated. Spectra were obtained in IRAffinity – Shimadzu spectrophotometer in diffuse reflection by ATR, the spectral range of 4000 to 400 cm<sup>-1</sup>, 4 cm<sup>-1</sup> resolution, and 32 scans.

## Physical properties (Cobb test, optical properties, air permeance, and roughness)

The water absorption capacity (Cobb test) was performed according to TAPPI T441 (2013) standard. This test expresses absorption capacity on a 1 m<sup>2</sup> paper surface. In this analysis, water absorption time was 60 seconds,

and the surface area of each sample was 25 cm<sup>2</sup>. Blotting paper of approximately 258 g/m<sup>2</sup> grammage was used. Cobb test was performed for all treatments in triplicate. The determination of the Cobb test was carried out following equation (5). Where: m<sub>1</sub> = Mass after water exposure (g); m<sub>0</sub> = Mass before water exposure (g).

$$\text{Water absorption capacity} \left( \frac{g}{m^2} \right) = (m_1 - m_0) * 400 \quad [5]$$

The optical properties of handsheets were performed by brightness and opacity determination. According to TAPPI T 452 (2008), analyses were carried out related to brightness, and TAPPI T 519 (2002) to opacity, in triplicate. A REGMED brightness meter with a directional reflectance level of 457 nm was used for analysis.

Air permeance and roughness were performed according to TAPPI T 460 (2006) and TAPPI T 538 (1996).

## Statistical analysis

A completed randomized design was performed for data analysis. The tested variables were bond strength (B), Cobb, Brightness, Opacity, Air permeance, and Roughness. The data homogeneity and normality were achieved. The results were evaluated by ANOVA and Tukey test ( $p < 0.05$ ). The statistical analyses were performed in SISVAR software (Ferreira 2011).

## Scanning electron microscopy

The structure analysis of handsheets was carried out using scanning electron microscopy (SEM). Virgin handsheets (T1, T2, and T3) and handsheets with 45:55 ratio (T6, T9, and T15) were submitted to SEM for evaluating physical structure and fiber arrangement. Analyses were carried out in Evo40 LEO XVP equipment with 25kV voltage. The handsheets were cut into tiny fragments for sample preparation. Samples were fixed in aluminum stubs, coated with aluminum foil film, double-sided carbon tape, and a thin gold layer was covered. Images were obtained in transversal and longitudinal sections.

# RESULTS AND DISCUSSION

## Bond strength

Interfiber bonding can be a weak spot in paper structure and be broken with simple hydration. However, they act decisively along with intrinsic fiber resistance to determine the paper mechanical properties, mainly tensile strength (Retulainen, 1997). Table 2 presents measured lab results and calculated data for parameters required for bond strength (B). Bond strength data presented a coefficient of variation of approximately 10.1% among replicates. Statistical differences occurred between treatments for bonding strength index. Results found in this study follow Area et al. (2010), who evaluated bond strength in eucalyptus Kraft pulps and obtained results around 12 N/mm<sup>2</sup>.

The highest B values were observed in treatments T1 (100E) and T10 (95E 5S), corresponding to higher eucalyptus content. The lowest B value was observed in treatment T19 (95S 5P), with sisal and pine blending. Expressive differences were noted comparing the three virgin pulps (T1, T2, and T3).

**Tab. 2** The tesing datasets.

Treatment	D (kg/m <sup>3</sup> )	G (g/m <sup>2</sup> )	FFI (N <sup>-1</sup> m <sup>-2</sup> )	RBA (%)	T (km)	Z (km)	L (cm)	A (cm <sup>2</sup> )	P (cm)	B (N/mm <sup>2</sup> )
T1 (100E)	399	67.3	1.02E+18	0.576	1.64	2.39	0.0881	2.5E-06	4.96E-03	12.73 a
T2 (100S)	382	63.2	7.2E+17	0.551	3.77	5.91	0.3566	3.17E-06	5.59E-03	6.95 efgh
T3 (100P)	427	66.4	1.52E+18	0.616	3.32	4.97	0.2807	3.96E-06	6.25E-03	8.84 bcde
T4 (5E 95S)	375	69.2	5.9E+17	0.541	3.35	4.79	0.3432	3.13E-06	5.56E-03	8.65 bcde
T5 (25E 75S)	401	59.1	1.06E+18	0.579	2.82	4.72	0.2895	3E-06	5.43E-03	5.13 fgh
T6 (45E 55S)	378	59.8	6.5E+17	0.546	2.52	4.19	0.2358	2.87E-06	5.31E-03	5.91 fgh
T7 (5E 95P)	450	64.1	1.94E+18	0.650	3.34	5.14	0.2711	3.89E-06	6.19E-03	7.98 cdef
T8 (25E 75P)	448	65.7	1.9E+18	0.646	3.41	5.15	0.2325	3.59E-06	5.93E-03	9.63 bcd
T9 (45E 55P)	437	67.4	1.7E+18	0.630	2.95	4.33	0.1940	3.3E-06	5.67E-03	10.81 ab
T10 (95E 5S)	410	61.8	1.22E+18	0.592	2.54	4.06	0.1015	2.53E-06	5.00E-03	13.03 a
T11 (75E 25S)	405	60.7	1.12E+18	0.584	2.70	4.41	0.1552	2.66E-06	5.12E-03	9.04 bcde
T12 (55E 45S)	413	64.0	1.27E+18	0.596	2.93	4.55	0.2089	1.37E-06	2.73E-03	7.68 cdefg
T13 (5S 95P)	490	67.2	2.66E+18	0.707	3.56	5.23	0.2845	3.92E-06	6.22E-03	8.62 bcde
T14 (25S 75P)	443	64.5	1.81E+18	0.639	3.46	5.36	0.2997	3.76E-06	6.09E-03	7.38 defg
T15 (45S 55P)	421	57.3	1.42E+18	0.608	3.15	5.47	0.3148	3.6E-06	5.95E-03	5.12 fgh
T16 (95E 5P)	438	64.3	1.72E+18	0.632	2.01	3.11	0.0977	2.57E-06	5.03E-03	10.99 ab
T17 (75E 25P)	446	64.6	1.86E+18	0.643	2.69	4.15	0.1362	2.86E-06	5.29E-03	11.01 ab
T18 (55E 45P)	460	66.3	2.11E+18	0.663	2.81	4.20	0.1748	3.16E-06	5.54E-03	10.04 bc
T19 (95S 5P)	397	53.3	9.9E+17	0.573	3.66	6.84	0.3528	3.21E-06	5.63E-03	4.68 h
T20 (75S 25P)	393	55.6	9.2E+17	0.568	3.56	6.33	0.3376	3.37E-06	5.76E-03	5.32 fgh
T21 (55S 45P)	411	61.8	1.24E+18	0.593	3.14	5.02	0.3224	3.52E-06	5.89E-03	5.95 fgh

Where: D=Sheet density, G=Grammage, FFI=Fiber flexibility index, RBA=Relative bonded area, T=Tensile index, Z= Zero-span tensile index, L= Fiber length, A= Average fiber cross section, P= Fiber cross section perimeter and B= Bond strength. Means followed by same letter in column do not differ statistically from each other by Tukey test at 5% probability level.

Bond strength in eucalyptus handsheets was approximately 83.1% and 44% higher than in sisal and pine handsheets, respectively. This result can suggest that eucalyptus fiber is more likely to connect to other fibers and increase fiber bonding. Generally, treatments containing eucalyptus in composition presented higher bond strength values, while treatments with sisal and pine presented lower values. As observed in Figure 1, increasing eucalyptus percentage in the blending tended to enhance bond strength values, both for sisal and pine blending, although eucalyptus and sisal blending fitted better. According to Zhang (2011), short fibers addition in blending, such as eucalyptus, improves interfiber bonding because the fibers act as connecting elements in the paper network.

Differences in fiber bonding strength can be related to fiber morphology since all materials presented discrepant fiber lengths. Eucalyptus fibers averaged approximately 880

µm in length while sisal and pine fibers averaged 3500 and 2800 µm, respectively. According to the Page equation, B and fiber length are indirectly related. Therefore, short fibers tend to present high bond strength values. Long fibers tend to present a reverse trend. Short fibers can bridge long fibers, contributing to bond connection and strength, improving the paper network. According to Larsson et al. (2018), long fibers present poor interfiber bonding and bond resistance.

Other factors can also affect fiber bond strength, such as refining. Increasing the refine degree can modify the B value since the bonding between fibers is enhanced (Dasgupta, 1994). However, considering that studied fibers were submitted to proper refining time, refining did not play a key role in bonding strength. Besides, bleaching, chemical content, and production process should also be considered (Area et al., 2010).

Some expressive B values are from fibers blending. They may be larger or equivalent to virgin fibers. This result can be due to the synergetic effect created when blending different fibers. Blended paper can show higher bond strength values than paper prepared with single fibers (Cappelletto et al., 2000; Danielewicz and Ślusarska, 2019).

The bond strength results can suggest that eucalyptus handsheets present better mechanical properties than the other fibers. Intermolecular interactions (Van der Waals' forces and hydrogen bonds) can occur with fiber bonding increment, contributing to internal cohesion and affecting paper properties (Vainio and Paulapuro, 2007). However, when it comes to strength properties, many other properties (fiber length, fiber flexibility, chemical content, fiber surface wettability, network structure, interlacement, and intrinsic

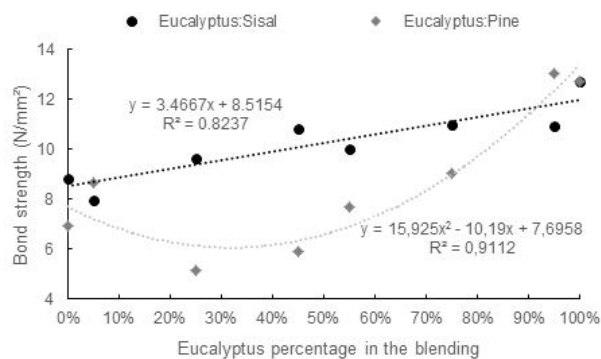


**Fig. 1** Bond strength behavior of blended paper with increasing of eucalyptus percentage.

fiber resistance.) should be considered. Therefore, bond strength is just indicative of mechanical properties. Perhaps, paper produced from sisal and pine fibers can present better strength properties than eucalyptus because of the better other properties, previously mentioned.

### Fourier Transform Infrared Spectroscopy

Figure 2 shows spectra of virgin pulp handsheets (T1, T2, and T3). The band located at  $3500\text{--}3100\text{ cm}^{-1}$  can be related to hydroxyl (OH) stretching vibrations, including water and other structures, mainly celluloses and hemicelluloses (Kazayawoko et al., 1997). The band at approximately  $1032\text{ cm}^{-1}$  can be related to C-O stretching. The band at  $2900\text{ cm}^{-1}$  can be assigned to C-H stretching (Huang et al., 2016). The band at  $1640\text{ cm}^{-1}$  can be assigned to double bond (C=C) or water adsorption. Bands between  $1400\text{--}1300\text{ cm}^{-1}$  are associated with C-H stretching and  $\text{CH}_2$  bending and rocking vibrations and related to cellulose crystallinity (Hajji et al., 2016).

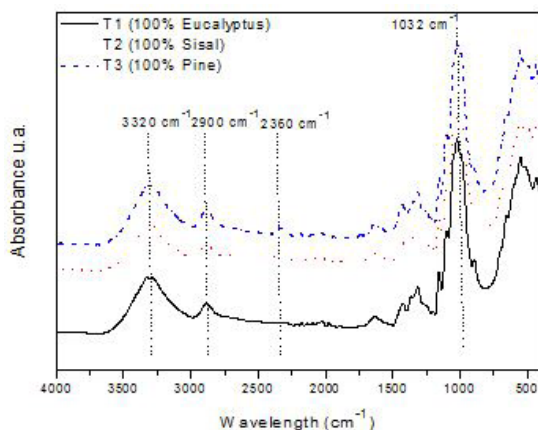


**Fig. 2** FTIR handsheet spectra from virgin pulps (T1, T2 and T3).

According to Figure 2, spectra from eucalyptus, sisal, and pine handsheets present a high similarity. Therefore, FTIR analysis was not sufficiently capable of discriminating chemical differences in handsheets. However, a few differences can be visualized between  $2170$  and  $2000\text{ cm}^{-1}$ . These differences can be associated with hemicellulose type or even different residual lignin content (Yang et al., 2006). The *Eucalyptus* spectrum did not present the band at  $2360\text{ cm}^{-1}$ , differently from sisal and pine spectra. This absorption peak can be assigned to the lignin structure, indicating that eucalyptus pulp obtained greater delignification when compared to the other materials (Puntambekar et al., 2016).

### Physical properties (Cobb test, optical properties, air permeance, and roughness)

Table 3 presents the results from the Cobb test, optical and other physical properties of blended paper. The cobb test shows the paper water absorption capacity. According to Table 3, all treatments presented great hydrophilicity. Handsheets presented no additive or charge added to their structure during formation or even modification in surface energy, probably changing

the hydrophilicity. Statistical differences occurred between treatments, which could be related to paper porosity and grammage, since these characteristics influence surface energy and wettability. However, an increasing or decreasing trend was not observed according to variation in material percentage. Bhardwaj et al. (2019) also detected no variation tendency in blending agro-residues and hardwood pulp.

The optical properties of paper have a massive importance in several applications and final destinations, such as newspaper, writing, and printing paper. The brightness and opacity are presented in Table 3 for all treatments. Some variables affect optical properties, like refining rate, residual lignin content, fines content, and factors related to form. Pulps used in this study have already been partially bleached but probably differed in chemical content, such as the residual lignin.

Evaluating Table 3, the highest brightness content was obtained in treatments with eucalyptus fiber in the blending, such as T1 (100E), T10 (95E 5S), and T16 (95E 5P). An increasing trend in paper brightness as eucalyptus percentage was enhanced in paper blending occurred, as evidenced in Figure 3. This can be explained because the original eucalyptus pulp possibly has a lower residual lignin content (which contributes to more significant brightness in mixtures with higher eucalyptus percentage). Cit (2013) also observed a brightness increment in blended paper with the increase of short eucalyptus fibers percentage in mixtures. On the other hand, the lowest brightness value was obtained in treatment T2 (100S), represented by 100% sisal. As the sisal proportion in the blending increased, a reduction in brightness occurred, as observed in Figure 3. This reduction is probably related to a high residual lignin content in the original sisal pulp. The lignin presents chromophore groups in the structure (Biermann 1996). Pine pulp (T3) presented high brightness compared to sisal pulp (T2), similar to that obtained by eucalyptus pulp. As a consequence, the brightness tended to increase with pine percentage increment in blending.

The addition of small quantities (25%) of eucalyptus and pine in sisal pulp enhanced pulp brightness by approximately 6 and 2 %, respectively. The use of fiber combination can be suitable when some application demands mechanical properties that sisal fiber can offer, like high tear strength and brightness appropriate for a particular situation.

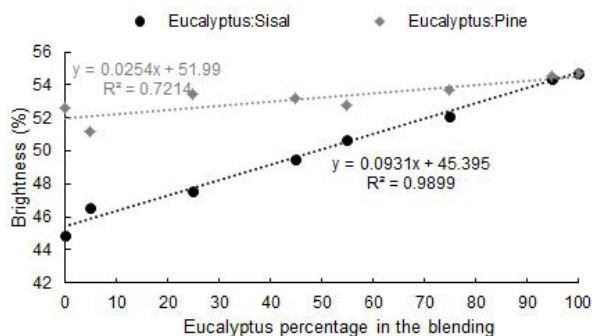


**Fig. 3** Brightness behavior of blended paper with eucalyptus percentage increment.



**Tab. 3** Cobb test, brightness, opacity, air permeance and roughness in each treatment.

Treatment	Cobb <sub>60</sub> (g/m <sup>2</sup> )	Brightness (%iso)	Opacity (%iso)	Air permeance µm/Pa·s	Roughness mL/min
T1 (100E)	138 ab (±8.5)	54.73 a (±1.53)	90.57 abc (±2.12)	110.65 a (±8.45)	1573 abc (±110)
T2 (100S)	140 a (±5.6)	44.90 i (±0.36)	92.57 a (±2.28)	42.37 cde (±2.61)	1943 ab (±161)
T3 (100P)	112 c (±2.8)	52.60 abc (±1.45)	82.03 g (±0.93)	38.26 cde (±1.89)	1536 abc (±169)
T4 (5E 95S)	136 abc (±5.6)	46.57 ghi (±0.38)	91.57 ab (±1.4)	44.66 cde (±5.82)	1925 ab (±115)
T5 (25E 75S)	118 abc (±8.4)	47.53 fghi (±1.25)	89.67 abcd (±2.06)	60.99 bcde (±2.19)	1315 bc (±32)
T6 (45E 55S)	120 abc (±5.6)	49.47 defg (±0.47)	89.50 abcd (±0.53)	45.37 cde (±7.09)	1462 abc (±55)
T7 (5E 95P)	114 bc (±2.8)	51.13 bcde (± 1.56)	82.47 g (±1.59)	24.79 e (±3.04)	1499 abc (±32)
T8 (25E 75P)	116 abc (±5.7)	53.47 ab (±0.4)	83.83 efg (±1.45)	28.43 de (±2.8)	1425 abc (±380)
T9 (45E 55P)	132 abc (±5.9)	53.17 abc (±1.36)	83.43 fg (±0.9)	53.8 bcde (±5.8)	1629 abc (±58)
T10 (95E 5S)	136 abc (±3.5)	54.37 a (±0.46)	88.67 abcd (±2.06)	68.72 bc (±7.93)	1555 abc (±115)
T11 (75E 25S)	138 ab (±2.8)	52.13 abcd (±1.19)	87.97 bcde (±0.85)	62.93 bcd (±2.7)	1462 abc (±166)
T12 (55E 45S)	132 abc (±1.9)	50.70 bcde (±0.26)	90.23 abcd (±0.59)	55.48 bcde (±5.78)	1962 ab (±123)
T13 (5S 95P)	118 abc (±7.6)	51.90 abcd (±1.47)	82.43 g (±1.72)	32.37 cde (±3.4)	2147 a (±134)
T14 (25S 75P)	120 abc (±2.3)	50.40 cdef (±0.44)	83.00 fg (±0.66)	31.45 cde (±2.37)	1610 abc (±89)
T15 (45S 55P)	116 abc (±5.7)	48.53 efgh (±0.55)	82.37 g (±1.86)	33.29 cde (±5.46)	1573 abc (±135)
T16 (95E 5P)	132 abc (±5.9)	54.50 a (±0.78)	87.97 bcde (±0.4)	66.89 bc (±1.25)	1092 c (±96)
T17 (75E 25P)	132 abc (±7.9)	53.73 ab (±1.0)	87.00 cdef (±1.42)	52.13 bcde (±4.41)	1240 bc (±102)
T18 (55E 45P)	126 abc (±8.4)	52.73 abc (± 0.75)	87.1 cdef (±0.62)	42.4 cde (±3.46)	1555 abc (±160)
T19 (95S 5P)	118 abc (±2.8)	44.67 i (± 1.12)	86.07 defg (±1.55)	86.92 ab (±2.96)	1740 abc (±168)
T20 (75S 25P)	114 bc (±2.8)	45.83 hi (±1.08)	86.30 cdefg (±1.4)	66.41 bcd (±1.83)	1795 abc (±110)
T21 (55S 45P)	114 bc (±3.0)	47.47 fghi (±0.45)	86.00 defg (±1.1)	34.21 cde (±3.76)	1518 abc (±134)
CV (%)	4.97	1.94	1.64	(±1.83)	15.86

Means followed by same letter in column do not differ statistically from each other by Tukey test at 5% de probability level.

The opacity is related to the spare capacity transmitted by paper and is an essential property for printing paper. This property suffers the influence of fibers network and its interlacement, besides physical properties (grammage and thickness), bleaching and filling materials. According to Table 3, there was a statistical difference among treatments. Materials with greater opacity were treatments with sisal and eucalyptus in their composition. Likely, eucalyptus presented high opacity due to their short fibers and the possibility of connections in the fiber network, making the material very compact and hindering light passage. Sisal behavior can be due to good handsheet compaction or, most likely, the impact of a process variable in handsheet forming like grammage and apparent density. The lowest opacity values were obtained in treatment T3 and others treatments involving pine pulp in composition. This can be related to fiber properties, such as high length and width, affecting handsheet forming and fiber interlacement.

The values of optical properties, both for brightness and opacity, are in concordance with others studies that evaluated the effect of fiber blending in these properties (Veisi and Mahdavi, 2016; Fathi and Kasmani, 2019; Bhardwaj et al., 2019).

Air permeance is a vital paper property and refers to the facility of air volume pass-through paper structure. Air permeance affects many applications such as food packaging, barrier properties, and filter paper. Air permeance is also related to empty spaces in paper structure and, consequently, permeability, since this property depends on the number, size, distribution, and pores format. According to Ek et al. (2009), air permeance is an indicator of paper structure controlled by pore volume, diameter, and network connectivity. Paper

with a low air permeance value is less porous and more resistant to air passage. They could be used in the paper that requires barrier properties such as waterproof paper and food packaging. On the other hand, paper with high air permeance could be used in other paper applications such as tissue, cardboard, writing, and printing paper.

According to Table 3 and Figure 4, statistical differences occurred among treatments. Highest values of air permeance were obtained in T1 (100E - 110,65 µm/Pa.s) and T19 (95S 5P - 86,92 µm/Pa.s), while lowest values were obtained in T7 (5E 95P - 24,79 µm/Pa.s) and T8 (25E 75P - 28.43 µm/Pa.s). The highest values corresponded to treatments containing eucalyptus, while the lowest values corresponded to pine treatments. The differences can be related to fiber morphology between fibers and how these affect fiber accommodation during handsheet forming and, consequently, paper structure. Generally, paper produced from long fibers tends to present high air permeance values compared to short fibers. Short fibers remain more compacted during forming and can present better interfiber bonding, reducing porosity and permeability. Laukala et al. (2019) reported an air permeance decrease with the addition of short hardwood fibers in blending with long softwood fibers. However, such a tendency was not presented in the studied paper. This behavior could be due to the influence of handsheet forming conditions (variations in fiber accommodation and physical properties), fiber morphological properties, or even poor fiber connections due to insufficient refining or specific pulp characteristic.

A clear tendency to increase or decrease fiber proportion in blending was not presented for air

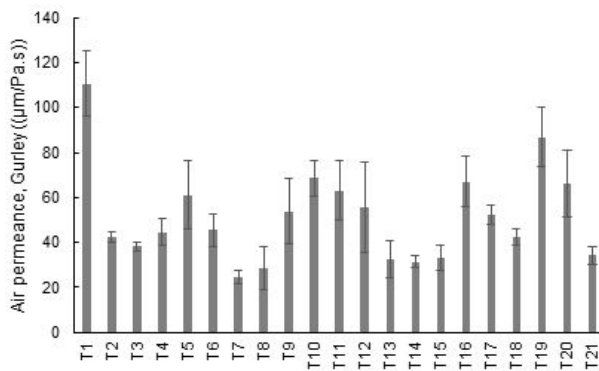


**Fig. 4** Air permeance behavior in each treatment.

permeance, except for eucalyptus addition. In summary, short eucalyptus fiber presented high air permeance (T1). As eucalyptus content increased in fiber blending, the air permeance tended to enhance blending with sisal and pine fibers, as observed in Figure 5. Cit (2013) also found air permeance increase with eucalyptus pulp addition in pine pulp, raising the possibility of air passage as the number of short fibers in blending increases. According to the author, eucalyptus addition affected the fiber interlacing network generating more spaces in a three-dimensional analysis. On the other hand, Zañão et al. (2019) found no air permeance with blending eucalyptus and pine fibers.

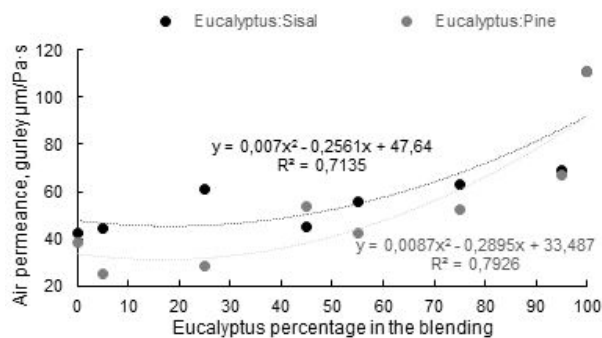


**Fig. 5** Air permeance behavior of blended paper with eucalyptus percentage increment.

The paper roughness expresses irregularities on paper structure numerically and affects the performance and paper applications. For example, writing, printing, and absorbent paper require an appropriate smoothness level, while other paper applications do not require much. According to Table 3 and Figure 6, statistical differences occurred among treatments. Highest values were obtained in T13 (5S 95P – 2147 mL/min), T12 (55E 45S – 1962 mL/min), T2 (100S – 1943 mL/min) and T4 (5E 95S – 1925 mL/min), while lowest values were obtained in T16 (95E 5P – 1092 mL/min) and T17 (75E 25P – 1240 mL/min). No tendency was observed with ratio variation in fiber blending for roughness. Fiber blending and morphologic fiber features had a small influence on roughness. Differences can be related to variation in fiber accommodation that occurred during the handsheet forming step. Neither additive nor

collage product was added to the handsheet structure or surface. This addition could have affected paper roughness. However, the highest values were correspondent to sisal and pine fibers. According to Omari et al. (2017), paper roughness is related to the long fiber presence in blends due to fiber conformability. Long agave fibers lead to the highest surface roughness and found in this study for sisal and pine fibers. Gülsoy and Pekközlü (2019) reported the same behavior. Short and fine fibers tend to present smaller roughness due to better conformability. The same authors also stated the influence of vessel elements on roughness.

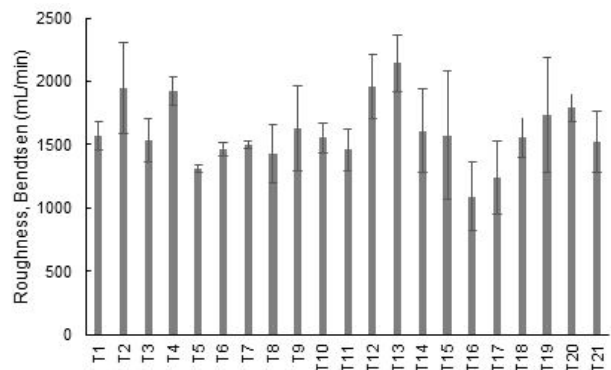


**Fig. 6** Roughness behavior in each treatment.

**Scanning electron microscopy (SEM)**

SEM analysis is essential when working with different fiber blending. Some characteristics seen in SEM images affect other paper properties, such as strength and physical properties. Morphological features, individual fiber strength, arrangement, and interfiber bonding are the most important factors affecting these paper properties (Page, 1969; Mossello et al., 2010).

Figures 7 and 8 show SEM images of transversal and longitudinal sections from virgin and blended handsheets. Virgin handsheets (T1, T2, and T3) were treatments with just one fiber type in paper structure. Blended handsheets (T6 - 45E 55S, T9 - 45E 55P, and T15 - 45S 55P) were treatments with the blending of two fibers combined with eucalyptus sisal and pine fibers at a 45/55 ratio. Differences are observed in the transversal section of handsheets (Figure 7) mainly related to morphological properties. As expected, blended paper (T6, T9, T15) presented an intermediate structure compared to virgin paper (T1, T2, and T3).

According to figure 7, fibers were thin and short in T1 as expected for eucalyptus fibers and presented vessel elements on the surface. Vessel elements can bring poor mechanical features to paper since they can act as a weak link due to low individual strength and connections (Zhao et al., 2019). T1 also presented voids in paper structure and more scattered fibers. This can suggest density decrease and porosity increase in handsheets (Vallejos et al., 2016). Porosity increase can be checked in Table 3. T1 and other treatments with eucalyptus content obtained high values of air permeance. T1 presented a more irregular structure which could affect physical properties such as thickness. As a result, T1 seemed to be thicker than other treatments, as observed in Figure 8.

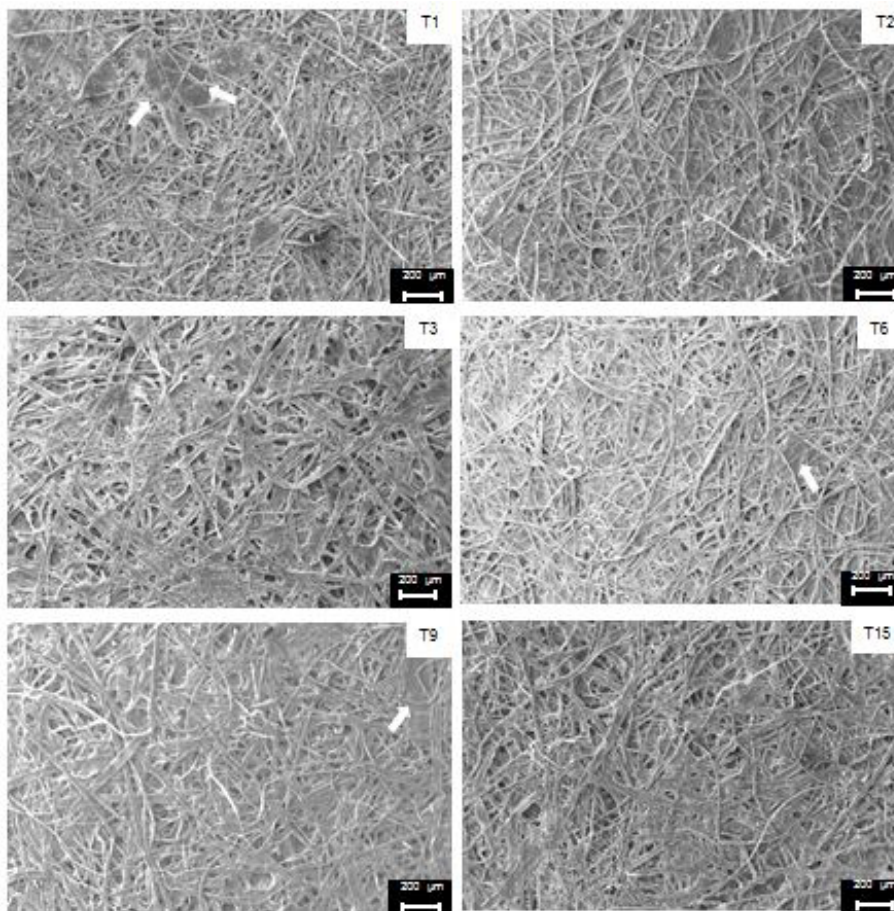


**Fig. 7** Scanning electron micrographs of handsheets surface from T1, T2, T3, T6, T9 and T15 at 100x magnification (arrows show vessel elements).

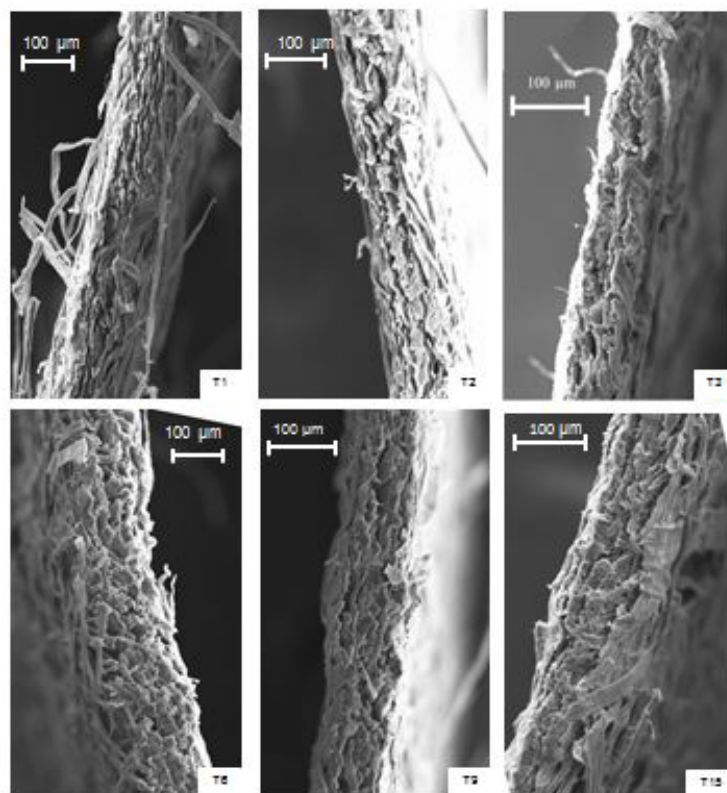


**Fig. 8** Scanning electron micrographs of handsheets cross-section from T1, T2, T3, T6, T9 and T15 at 300x magnification.



Fibers presented similar width in T2 as observed in T1. However, the fiber length was dramatically different. T2 fibers were quite long and can probably contribute to paper strength. Although more minor than T1, T2 also presented voids in paper structure, reflecting density and porosity. On the other hand, T2 seemed to be more compact, as observed in Figures 7 and 8. Such behavior can affect thickness and density. A compacted paper may also present appropriated strength property due to better stress transfer during the requests (Tabarsa et al., 2017). T2 structure is better distributed and oriented, making it a more closed structure. This can be due to better fiber accommodation in handsheet forming and morphological properties. T2 also presented a more stable structure, increasing surface uniformity (less coarse and more collapsed surface). The surface uniformity may have contributed to handsheet roughness (Table 3). The highest roughness values were obtained in treatments containing sisal fibers. According to Banerjee et al. (2009), SEM images can determine surface roughness measurements of paper since this technique can detect subtle changes in sheet structure.

T3 fibers seen in Figures 7 and 8 presented a large width compared to T1 (eucalyptus) and T2 (sisal fibers). Also, fibers presented great lengths, higher than T1 and lower than T2. This is a well-known characteristic of some conifer's fiber. Morphological properties of pine fiber can contribute to better strength properties. As well as T2, T3 presented a compacted structure due to better interfiber bonding, better accommodation, and flexibility. T3 presented the lowest thickness, according to Figure 8. Fibers seemed to be flat compared to the other fibers, which could have contributed to fiber flexibility, affecting thickness, interfiber bonding, and fiber-to-fiber interaction (Kim et al., 2014). According to Karademir et al. (2004), flat fiber is expected to create a larger contact area between fibers, better conformation, and stronger resultant paper.

As already pointed out, SEM images from blended paper (T6, T9, and T15) presented different features compared to virgin paper. These features were a compilation of virgin characteristics. In other words, T6, T9, and T15 presented the intermediate behavior of the two fibers that made up the blending. For example, blending with eucalyptus presented some vessel elements, thin and short fibers in paper structure, and other different fibers. According to Figures 7 and 8, fiber blending affected paper properties seen by SEM images, and differences can reflect in interfiber bonding, surface uniformity, fiber arrangement, physical and strength properties. Therefore, paper properties could be improved depending on fiber blending, and proper properties from each pulp could be engineered to a specific situation/application, as observed in T15 by SEM images. T15 was sisal and pine blending and presented suitable features from each fiber.

Consequently, T15 seemed to be more compacted due to better fiber accommodation/interfiber bonding, improving connections between fibers and reflection in thickness. Fibers were better distributed and arranged, presenting few voids in structure. This could probably affect porosity, as observed in Table 3. The surface was also uniform, reflecting in roughness. Handsheet properties observed in SEM images suggested that T15 can present better strength properties.

Even interfiber bonding can be improved with fiber blending. Motamedian et al. (2019) observed by SEM images occurrence and formation of bridges/connections among morphologically different fibers. However, fiber blending can also bring different consequences depending on fiber type. Aqeela et al. (2018) observed by SEM images the effect of fiber blending in thickness. Blended papers were approximately 2x thicker than virgin paper. Besides, the blended paper was less uniform due to differences in fiber shapes and dimensions.

## CONCLUSIONS

This study investigated the effect of different fiber blending in bond strength, physical, optical, and structural properties. Statistical differences occurred among blended and virgin handsheet for all properties. In some cases, blended handsheet was higher than respective virgin handsheets, highlighting the synergetic effect. Treatment T15 (45S 55P) presented the best results and possible better physical-mechanical properties due to the morphological properties of the fibers.

Treatments containing eucalyptus fibers presented higher bond strength values. An increasing trend was observed as eucalyptus percentage enhanced in blending. The lowest values were obtained in sisal and pine handsheets. In general, eucalyptus handsheets were 83.1% and 44% higher than sisal and pine for bond strength. FTIR spectra showed similarity between the three different virgin handsheets. Differences were related to 2170-2000  $\text{cm}^{-1}$  and 2360  $\text{cm}^{-1}$  peak, probably related to chemical content in pulps, especially residual lignin. All treatments presented great hydrophilicity. No tendency was observed in the Cobb test. *Eucalyptus* and *Pinus* treatments presented high brightness. *Eucalyptus* fiber addition in blending caused a brightness increase in blended handsheets, as well as pine addition. Small eucalyptus and pine fiber concentration additions in sisal pulp can enhance paper brightness. Sisal and eucalyptus treatments presented high opacity, while pine treatments presented opposite results. *Eucalyptus* treatments also presented high air permeance values. The increasing tendency was reported in sisal and pine blending for air permeance. The highest roughness values were obtained in sisal and pine treatments, probably due to their long fibers. SEM images revealed differences between handsheets regarded fiber morphological properties.

## ACKNOWLEDGMENTS

Authors would like to thank Klabin and Lwarcell S.A, Instituto de Pesquisas Tecnológicas – IPT and Universidade Federal de Lavras. This research was financed in part by the Coordenação de Aperfeiçoamento de Pessoal de Nível Superior – Brazil (CAPES) – Finance Code 001.

## REFERENCES

- AQEELA, M. Y. N.; AINUN, Z. M. A.; JAWAID, M. Effect of pretreatment concentration on pulp blending between oil palm empty fruit bunch and citronella leaf fibers in terms of pulp and paper properties. *Wood Biofiber Int Conf.* v. 368, 012010, p.1-9, 2018.
- AREA, M. C.; BENITEZ, J.; FELISSIA, F. E. Componentes da resistência à tração de polpas kraft de *Eucalyptus grandis*. *O Papel*, v. 71, p. 48–62, 2010.

- BANERJEE, S.; YANG, R.; COURCHENE, C. E.; CONNERS, T. E. Scanning electron microscopy measurements of the surface roughness of paper. *Ind Eng Chem Res*, v. 48, p. 4322–4325, 2009.
- BHARDWAJ, S.; BHARDWAJ, N. K.; NEGI, Y. S. Cleaner approach for improving the papermaking from agro and hadwood blended pulps using biopolymers. *J Clean Prod*, v. 213, p. 134–142, 2019.
- BIERMANN, C. J. *Handbook of pulping and papermaking*. Academic Press, San Diego, 1996.
- CAPPELLETO, P.; MONGARDINI, F.; BARBERI, B.; SANNIBALE, M.; BRIZZI, M.; PIGNATELLI, V. Papermaking pulps from the fibrous fraction of *Miscanthus x Giganteus*. *Ind Crops Prod*, v. 11, p. 205–210, 2000.
- CLARAMUNTA, J.; MAS, M. T.; PARDO, G. Mechanical characterization of blends containing recycled paper pulp and other lignocellulosic materials to develop hydromulches for weed control. *Biosystems Engineering*, v. 191, p. 35–47, 2020.
- CIT, E. J. Influência da mistura de fibras de *Eucalyptus dunni* M. e *Pinus taeda* L. de processo "Kraft" nas propriedades do papel. 2013. 154 p. PhD thesis, Universidade Federal do Paraná.
- DANIELEWICZ, D.; SURMA-SŁUSARSKA, B. Bleached Kraft pulps from blends of wood and hemp, part I. demand for alkali, yield of pulps, their fractional composition and fibre properties. *Fibres Text*, v. 27, p. 112–117, 2019.
- DASGUPTA, S. Mechanism of paper tensile-strength development due to pulp beating. *Tappi J*, v. 77, p. 158–166, 1994.
- EK, M.; GELLERSTEDT, G.; HENRIKSSON, G. *Paper products physics and technology*. Walter de Gruyter, 2009.
- FATHI, G.; KASMANI, J. E. Prospects for the preparation of paper money from cotton fibers and bleached softwood kraft pulp fibers with nanofibrillated cellulose. *BioResources*, v. 14, p. 2798–2811, 2019.
- GÜLSOY, S. K.; KILIÇ PEKGÖZLÜ, A. Influence of fiber fractionation on kraft paper properties of European black pine and European aspen. *Turkish J Agric For*, v. 43, p. 184–191, 2019.
- HAJJI, L.; BOUKIR, A.; PESSANHA, S.; FIGUEIRINHAS, J. L.; CARVALHO, M. L. Artificial aging paper to assess long-term effects of conservative treatment. Monitoring by infrared spectroscopy (ATR-FTIR), X-ray diffraction (XRD), and energy dispersive X-ray fluorescence (EDXRF). *Microchemical J*, v. 124, p. 646–656, 2016.
- HUANG, J.; ZHANG, L.; ZHOU, Y. et al. Study on the suitability of bamboo fiber for manufacturing insulating presspaper. *IEEE Trans Dielectr Electr Insul*, v. 23, p. 3641–3651, 2016.
- LARSSON, P. T.; LINDSTRÖM, T.; CARLSSON, L. A.; FELLERS, C. Fiber length and bonding effects on tensile strength and toughness of kraft paper. *J Mater Sci*, v. 53, p. 3006–3015, 2018.
- LAUKALA, T.; OVASKA, S. S.; TANNINEN, P.; PESONEN, A.; JORDAN, J.; BACKFOLK, K. Influence of pulp type on the three-dimensional thermomechanical convertibility of paperboard. *Cellulose*, v. 26, p. 3455–3471, 2019.
- KARADEMIR, A.; HOYLAND, R. W.; XIAO, H.; WISEMAN, N. A study on the effects of AKD and Ketone on paper sizing and friction. *Appita J*, v. 57, p. 116–119, 2004.
- KARLSSON, H. Strength properties of paper produced from softwood kraft pulp - pulp mixture, reinforcement and sheet stratification. 2010. 109 p. PhD thesis. Karlstad University Studies.
- KAZAYAWOKO, M.; BALATINECZ, J. J.; WOODHAMS, R. T. Diffuse reflectance fourier transform infrared spectra of wood fibers treated with maleated polypropylenes. *J Appl Polym Sci*, v. 66, p. 1163–1173, 1997.
- KIM, J.; JANG, D.; YOON, S.; SHIN, H.; PARK, J. Changes of handsheet fracture toughness by wood and cotton fibers mixing. *J Korea Tappi*, v. 46, p. 81–87, 2014.
- KMURA, M.; ISHIDA, T.; ONO, Y. Significant contribution of fibrils on pulp fiber surface to water retention value. *Nordic Pulp & Paper*, v. 35, n. 1, p. 96–105, 2020.
- MANSFIELD, S. D.; KIBBLEWHITE, R. P.; RIDDELL, M. J. C. Characterization of the reinforcement potential of different softwood kraft fibers in softwood/hardwood pulp mixtures. *Wood Fiber Sci*, v. 36, p. 344–358, 2004.
- MOSSELLO, A. A.; HARUN, J.; RESALATI, H.; IBRAHIM R.; SHMAS, S.; TAHIR, P. New approach to use of kenaf for paper and paperboard production. *BioResources*, v. 5, p. 2112–2122, 2010.
- MOTAMEDIAN, H. R.; HALILOVIC, A. E.; KULACHENKO, A. Mechanisms of strength and stiffness improvement of paper after PFI refining with a focus on the effect of fines. *Cellulose*, v. 26, p. 4099–4124, 2019.
- OMARI, H.; BELFKIRA, A.; BROUILLETTE, F. Paper properties of *Typha latifolia*, *Pennisetum alopecuroides*, and *Agave americana* fibers and their effect as a substitute for kraft pulp fibers. *J Nat Fibers*, v. 14, p. 426–436, 2017.
- PAGE, D. A theory for the tensile strength of paper. *Tappi*, v. 52, p. 674–681, 1969.
- PUNTAMBEKAR, R.; PYDIMALLA, M.; DINDA, S.; ADUSUMALLI, R. B. Characterization of Eucalyptus heartwood and sapwood pulp after kraft cooking. *J Indian Acad Wood Sci*, v. 13, p. 8–15, 2016.
- RETULAINEN, E. The role of fibre bonding in paper properties. 1997. 78 p. Dissertation. Helsinki University of Technology.
- SCHNEIDER, A.; GARCIA, D.; BRASILEIRO, J. G.; MAYER, V. G.; MISKE, A. S. W. Sustentabilidade e oportunidades para a indústria de papel na América Latina. *Rev FAE*, v. 1, p. 47–59, 2016.
- SHEIKHI, P.; ASADPOUR, G.; ZABIHZADEH, S. M.; AMOEE, N. An optimum mixture of virgin bagasse pulp and recycled pulp (OCC) for manufacturing fluting paper. *BioResources*, v. 8, p. 5871–5883, 2013.
- TABARSA, T.; SHEYKHNAZARI, S.; ASHORI, A.; MASHKOUR, M.; KHAZAEIAN, A. Preparation and characterization of reinforced papers using nano bacterial cellulose. *Int J Biol Macromol*, v. 101, p. 334–340, 2017.
- TAO, J.; LIU, H. A method to determine sheet relative bonded area using the fiber flexibility index. *Instrum Sci Technol*, v. 39, p. 161–172, 2011.
- TAPPI - Technical Association of the Pulp and Paper Industry- TAPPI test methods.
- VAINIO, A. K.; PAULAPURO, H. Interfiber bonding and fiber segment activation in paper. *BioResources*, v. 2, p. 442–458, 2007.
- VALLEJOS, M. E.; FELISSIA, F. E.; AREA, M. C.; EHMAN, N. V.; TARRES, Q.; MUTJE, P. Nanofibrillated cellulose (CNF) from eucalyptus sawdust as a dry strength agent of unrefined eucalyptus handsheets. *Carbohydr Polym*, v. 139, p. 99–105, 2016.
- VEISI, A.; MAHDAVI, S. Mixing bleached white poplar and wheat straw chemimechanical pulps to improve the mechanical and optical characteristics. *BioResources*, v. 11, p. 2987–2997, 2016.
- YAN, D.; LI, K. Evaluation of inter-fiber bonding in wood pulp fibers by chemical force microscopy. *J Mater Sci Res*, v. 2, p. 23–33, 2013.
- YANG, H. et al. Characteristics of hemicellulose, cellulose and lignin pyrolysis. *Fuel*, v. 86, p. 1781–1788, 2006.
- ZANÃO, M.; COLODETTE, J. L.; OLIVEIRA, R. C. ALMEIDA, D.; GOMES, F. J. B.; CARVALHO, D. Evaluation of kraft-PS cooking for eucalypt and pine wood chip mixtures. *J Wood Chem Technol*, v. 39, p. 149–165, 2019.
- ZHANG, H.; HE, Z.; NI, Y. Improvement of high-yield pulp properties by using a small amount of bleached wheat straw pulp. *Bioresour Technol*, v. 102, p. 2829–2833, 2011.
- ZHAO, X.; GUO, P.; PENG, H.; ZHAO, P.; YANG, Y.; ZHANG, Z. Potential of Pulp production from whole-tree wood of *Betula platyphylla* Roth. based on wood characteristics. *BioResources*, v. 14, p. 7015–7024, 2019.